УДК [681.7.01+66.088+615.478.6]

JIAO HUNKUN, OLEH AVRUNIN

EXPLORE THE FEASIBILITY STUDY OF MAGNETIC STEREOTAXIC SYSTEM

Kharkiv National University of Radio Electronics, Kharkiv, Ukraine, 1350829683@qq.com, jiaohankun19921208@gmail.com, jiao.hankun@nure.ua,

Анотація. У цій статті детально представлено систему магнітного стереотаксису та встановлено базову модель магнітної стереотаксичної системи в тривимірному просторі за допомогою програмного забезпечення для комп'ютерного моделювання COMSOL, а також проведено теоретичний аналіз та експерименти з комп'ютерного моделювання безконтактного керування імплантатами. Після цього рейкова система, керована Arduino, була побудована в реальних експериментах, а результати експериментів комп'ютерного моделювання були перевірені. Також було продемонстровано, що зміна напруженості зовнішнього магнітного поля в магнітній стереотаксичній системі дозволяє безконтактно контролювати рух імплантату.

Ключові слова: здоров'я людини, магнітне поле, програмне забезпечення COMSOL, постійні магніти, мікроконтролери Arduino

Abstract. This paper introduces the magnetic stereotaxis system in detail, and establishes the basic model of the magnetic stereotaxic system in three-dimensional space through the computer simulation software COMSOL, and conducts theoretical analysis and computer simulation experiments on the non-contact control of implants. After that, the slide rail system controlled by Arduino was constructed in actual experiments, and the results of computer simulation experiments were verified. It has also been demonstrated that changing the external magnetic field strength in a magnetic stereotaxic system enables non-contact control of implant movement.

Keywords: Human health, Magnetic field, COMSOL Software, Permanent magnets, Arduino microcontrollers

DOI: 10.31649/1681-7893-2023-45-1-86-96

I. INTRODUCTION TO MAGNETIC STEREOTAXIC SYSTEMS

Magnetic stereotaxic system[1-3] is a new type of high-precision neurosurgical system in the experimental research stage. The idea is to guide small magnetic surgical instruments into the skull through a catheter through an external magnetic field, follow the pre-operative pre-designed and calculated trajectory to reach the deep structure of the brain tissue, provide hyperthermia to the lesion located in the deep structure of the brain tissue, or deliver drugs through the catheter.

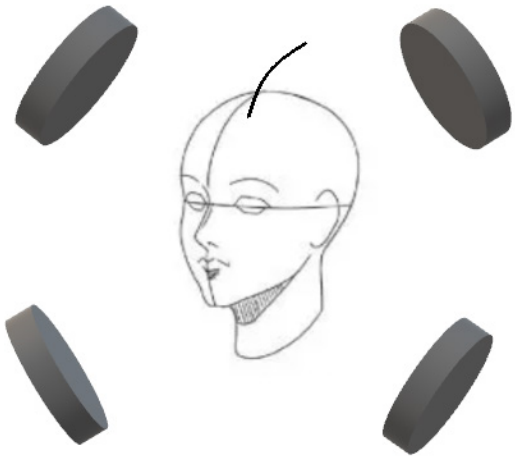

Figure 1 – Basic schematic diagram of magnetic stereotaxic system

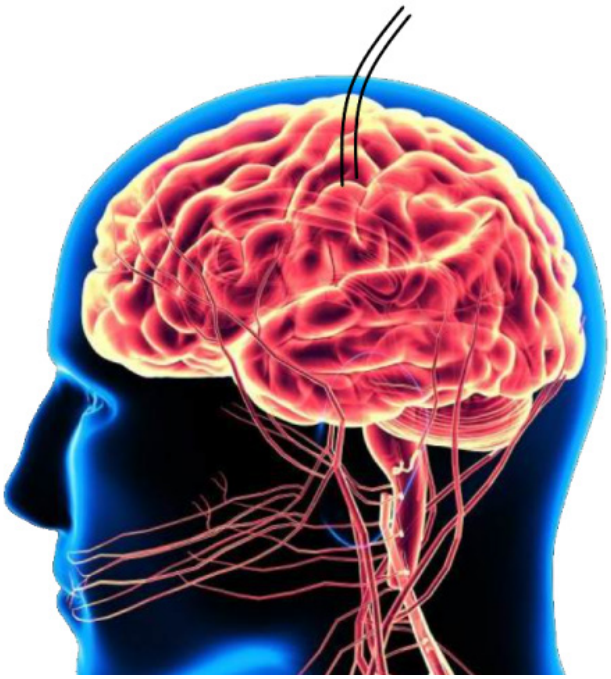

Figure 2 – Schematic diagram of magnetic implants with catheter connections into brain tissue

In traditional intracranial neurosurgery, neurosurgical intervention is typically performed using stereotaxic devices with mechanically controlled surgical instruments that can only move along a straight trajectory [4-8].However, this method has limited surgical access and is difficult to enter the deep structure of brain tissue, because the surgical instruments can only move in a straight trajectory, so the trauma to the tissues on the movement path and the surrounding tissues of the lesion is high, and it cannot effectively treat many diseases of the brainstem tumor and extrapyramidal nervous system.

Compared to traditional treatments, magnetic stereotaxic systems provide non-contact control of the implant by changing the external magnetic field, so through pre-design and calculation, multiple surgical pathways can be established, which allows the implant to reach almost any area of brain tissue along any trajectory to ensure minimal trauma to the surrounding tissues of the movement path and lesions. This also makes the magnetic stereotaxic system one of the least invasive methods for surgical intervention on lesions located in the brain.

II. SIMULATION EXPERIMENT OF MAGNETIC STEREOTAXIC SYSTEM

The magnetic stereotaxic system controls the implant movement through the change of the external magnetic field, so in the simulation experiment, we use a large permanent magnet to form an external magnetic field, and a small permanent magnet is used as an implant for simulation modeling. The simulation software chose COMSOL 6.0[9,10].

1**. Experimental design:** Establish a three-dimensional space coordinate system in the software, set the small permanent magnet in the center of the three-dimensional space, and set the large permanent magnet on the +X, +Y, -X, -Y axis respectively, that is, four large permanent magnets facing each other constitute an external magnetic field, and the small permanent magnet is an implant[11-13]. After that, parameters are set in the COMSOL software based on real material data used in the experiment, and a geometric model is constructed.

2. The parameters are set as follows:

(1) Large permanent magnet diameter d_ion=100[mm]=0.1[m];

(2) Large permanent magnet thickness t_ion=20 [mm]=0.02[m];

(3) Small permanent magnet diameter d_NFB =1[mm]=0.001[m];

(4) Small permanent magnet thickness l_NFB=2[mm]=0.002[m];

(5) The movement boundary of the small permanent magnet is a cylinder with a radius of 0.1 [m] and a height of 0.4 [m];

(6) The closest distance of large permanent magnets from the center position is 0.12m, and the maximum distance is 0.43m, that is, the movable distance of large permanent magnets is 0.3m.

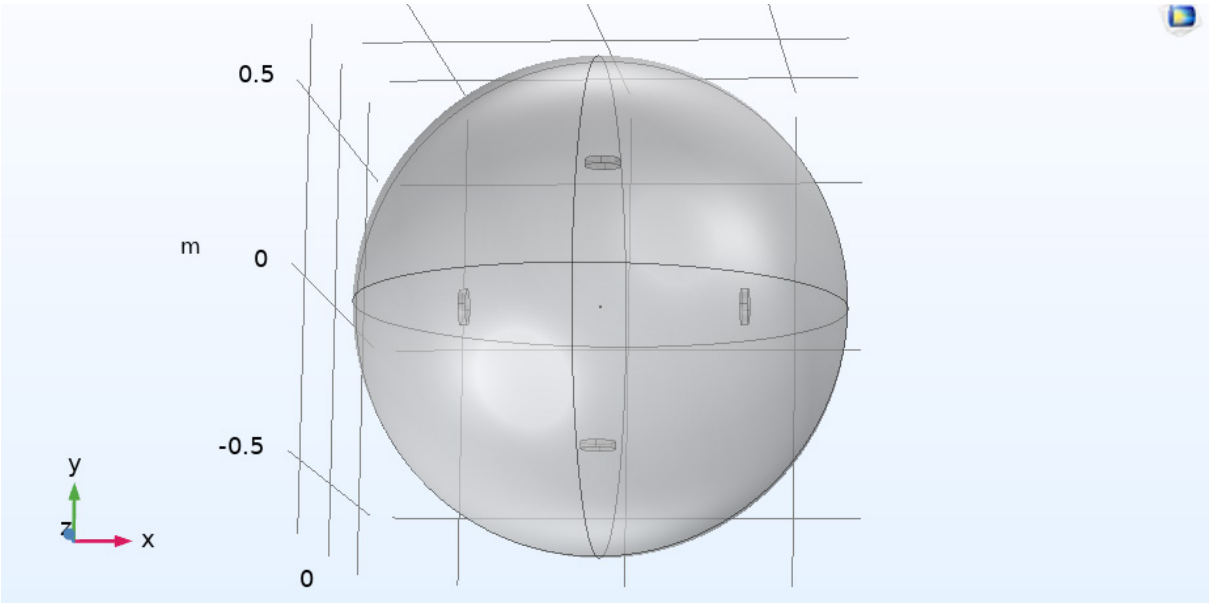

Figure 3 – Geometric model of a magnetic stereotaxic system in 3D space.

Since the external magnetic field consists of a large permanent magnet that can be moved, and the magnetic field generated by the permanent magnet is a constant static magnetic field, we select "Magnetic field, no current (mfnc)" in the AC/DC module when setting the physics field. The material parameters of the model are set as follows:

3. NdFeB magnet[19](Permanent magnets) :

(1) Conductivity σ=1/1.4[uohm*m][S/m];
(2) Relative permittivityεr=1 [1];
(3) Recovery permeability μrec=1.02;
(4) Residual flux density norm normBr=1.3[T];

4. Perimeter space (air) :

(1) Conductivity σ=0[uohm*m][S/m];
(2) Relative permittivityεr=1 [1];
(3) Recovery permeability μrec=1;

All of the above parameters are assignments and can be changed according to the specific situation of the experimental material.

5. Equations and formulas used in simulation experiments

Magnetostatics is the subfield of electromagnetics describing a static magnetic field, such as the one generated by a steady electric current or a permanent magnet. Starting with free space, the equations of magnetostatics are Gauss's magnetic law:

$$\nabla \cdot \mathrm{B} = 0 \tag{1}$$

and Maxwell–Ampère's law (static version)[14]:

$$\nabla \times \mathrm{B} = \mu_0 \mathrm{J} \tag{2}$$

where $\mathbf{B}$ is the magnetic flux density, $\mathbf{J}$ is the current density, and μ_0 is the permeability of vacuum.

Note that the magnetic version of Gauss's law implies that there are no magnetic charges. A further consequence of this law is that the magnetic flux density is solenoidal, or divergence free. This means that the field can be written as the curl of another vector field as follows:

$$\mathrm{B} = \nabla \times \mathrm{A} \tag{3}$$

where the field $\mathbf{A}$ is called the magnetic vector potential.

The electric potential allows for a more efficient way of expression for the equations of electrostatics and steady currents. In a similar way, the magnetic vector potential allows for a more efficient way of formulating the equations of magnetostatics, as shown further below.

Helmholtz's theorem says that a vector field is defined (up to a constant) by its curl and divergence. The choice of divergence of the magnetic vector potential is nontrivial. One of several choices is the Coulomb gauge:

$$\nabla \cdot \mathbf{A} = 0 \tag{4}$$

Using the magnetic vector potential, the equations of magnetostatics in free space can be combined into one equation:

$$\nabla \times \nabla \times \mathbf{A} = \mu_0 \mathbf{J} \tag{5}$$

The vector identity:

$$\nabla \times \nabla \times \mathbf{A} = \nabla(\nabla \cdot \mathbf{A}) - \nabla^2 \mathbf{A} \tag{6}$$

Permanent magnets have a permanent magnet moment, therefore, the magnetic flux density in permanent magnets and in free space is different, in order to describe this phenomenon macroscopically, the magnetization vector field **M** and the magnetic field strength **H** are introduced, the relationship is as follows:

$$\mathbf{H} = \frac{\mathrm{B}}{\mu_0} - \mathrm{M} \tag{7}$$

where μ_0 is the magnetic permeability.

For a situation where there are no free currents, but only a magnetization vector field, Maxwell–Ampère's law takes the simplified form:

$$\nabla \times (\frac{1}{\mu_0}\mathrm{B} - \mathrm{M}) = \nabla \times \mathbf{H} = 0 \tag{8}$$

The fact that the magnetic intensity field is irrotational (curl free) means that a scalar potential exists (say, V_m), such that:

$$\mathrm{H} = -\nabla \mathrm{V_m} \tag{9}$$

This can be combined with Gauss's magnetic law and:

$$\mathrm{B} = \mu_0(\mathrm{H} + \mathrm{M}) \tag{10}$$

to get the following equation for magnetostatics with no free currents:

$$-\nabla \cdot (\mu_0(\nabla V_m + \mathrm{M})) = 0 \tag{11}$$

In constitutive relations B-H, for the magnetization model, choose the residual flux density formula:

$$\mathbf{B} = \mu_0 \mu_{rec} \mathbf{H} + \mathbf{B_r}$$
$$\mathbf{B_r} = \|\mathbf{B_r}\| \frac{\mathbf{e}}{\|\mathbf{e}\|}$$

Where B is the magnetic flux density, μ_0 is the vacuum permeability, μ_{rec} is recoil permeability, B_r is residual flux density, $\|B_r\|$ is residual flux density norm, e is residual flux direction.

6. SIMULATION EXPERIMENT RESULTS

Magnetic field strength distribution of large permanent magnets at a distance of 400 [mm] from the center of three-dimensional space.The cylinder in the middle indicates the range of movement of the implant within the skull.

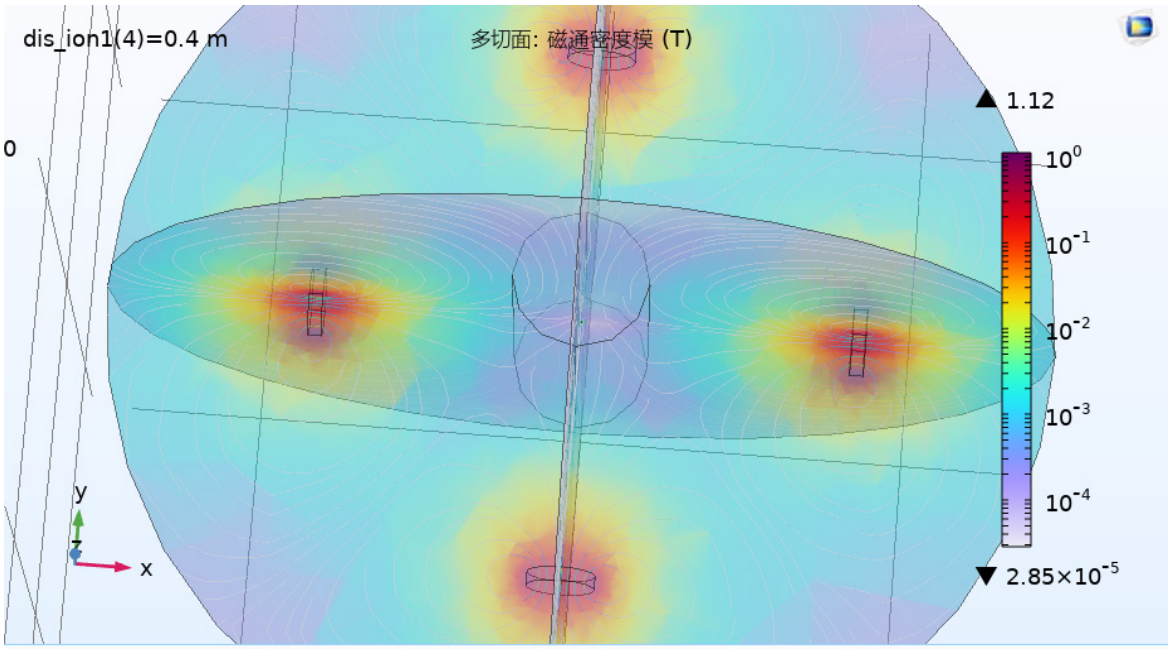

Figure 4 – Schematic diagram of magnetic field strength of magnetic stereotaxic system.

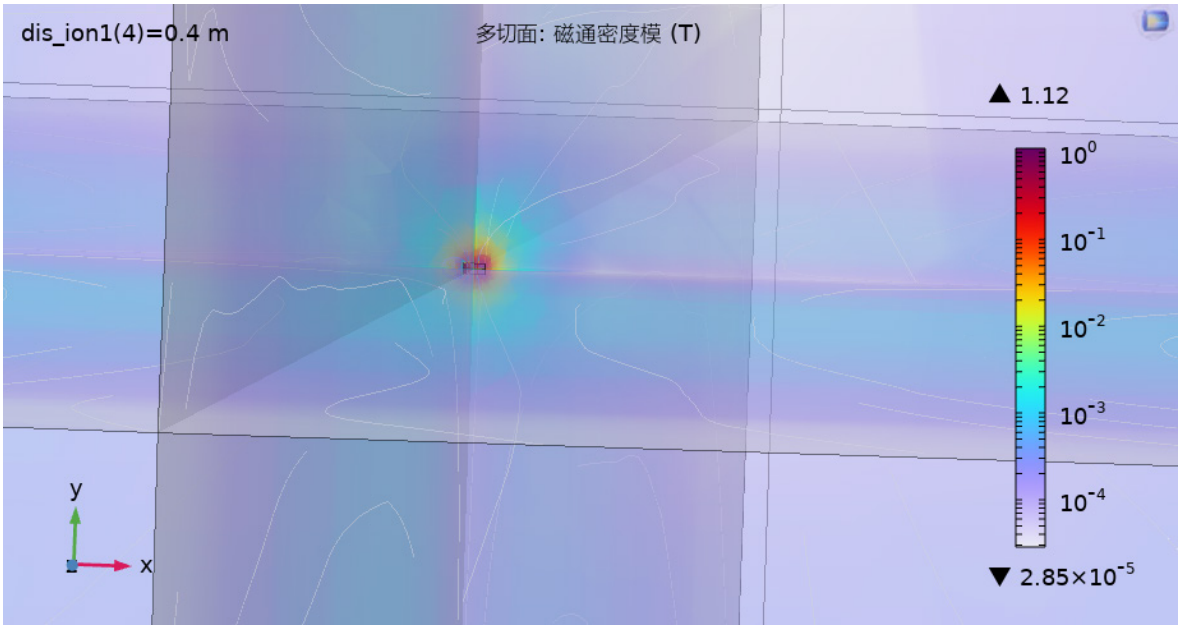

Figure 5 – Distribution of magnetic field strength around small permanent magnets..

When a large permanent magnet located on one side begins to move toward the center position, its magnetic field begins to gradually contact the small permanent magnet.

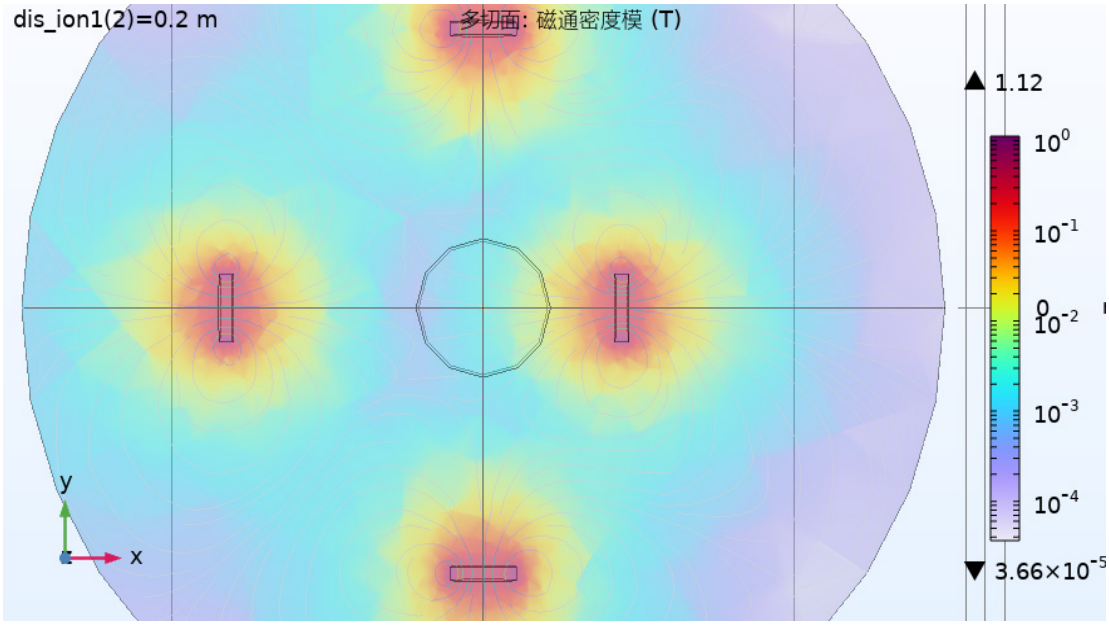

Figure 6 – Schematic diagram of the magnetic field strength of a large permanent magnet on one side moving 0.2 [mm] from the center of three-dimensional space.

Since the magnetic field of a large permanent magnet gradually touches the small permanent magnet during its movement, we use the "Force Calculation" module included with the software to analyze the force of the small permanent magnet.

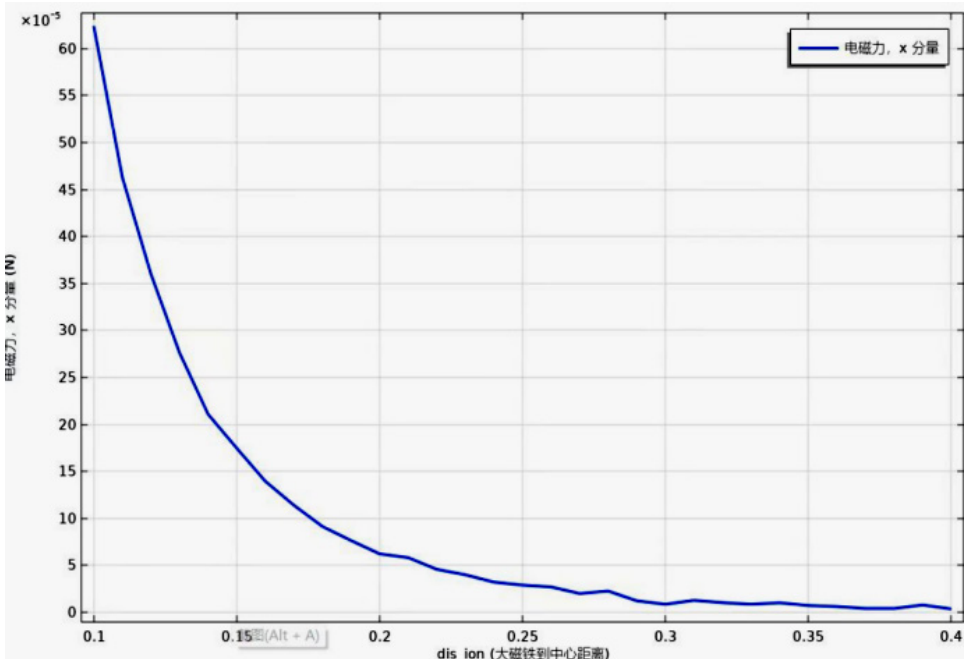

Figure 7 – When a large permanent magnet located on the +X axis moves toward the center, stress analysis of small permanent magnets.

Through the stress analysis of small permanent magnets, we find that when the large permanent magnets on one side gradually approach, the small permanent magnets are attracted by the large permanent magnets, will move towards the direction of the large permanent magnets, and stay at the boundary after being blocked by the boundary.As the large permanent magnet gradually leaves, the small permanent magnet remains at the boundary position.

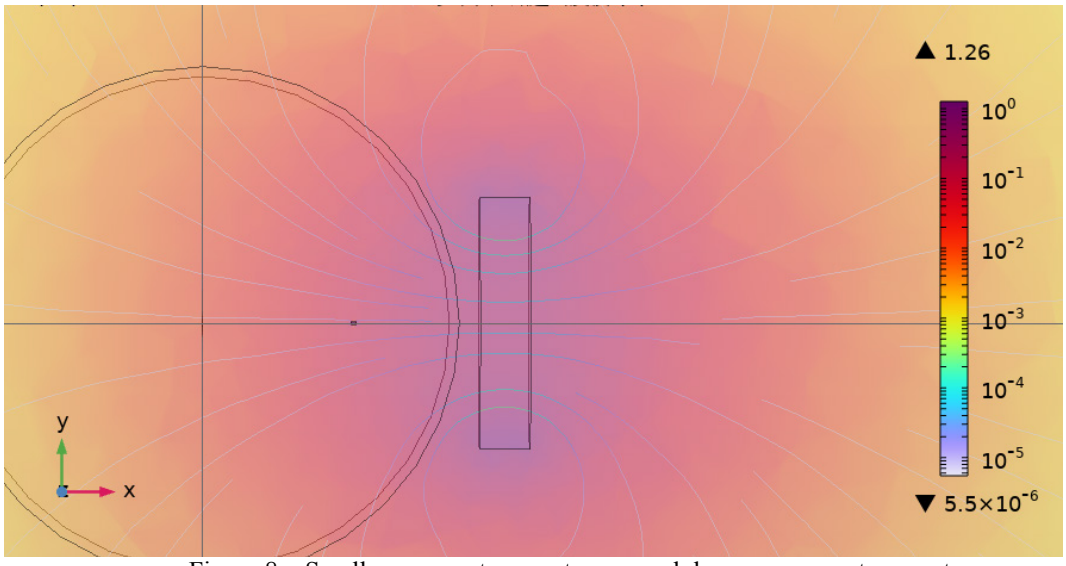

Figure 8 – Small permanent magnets approach large permanent magnets.

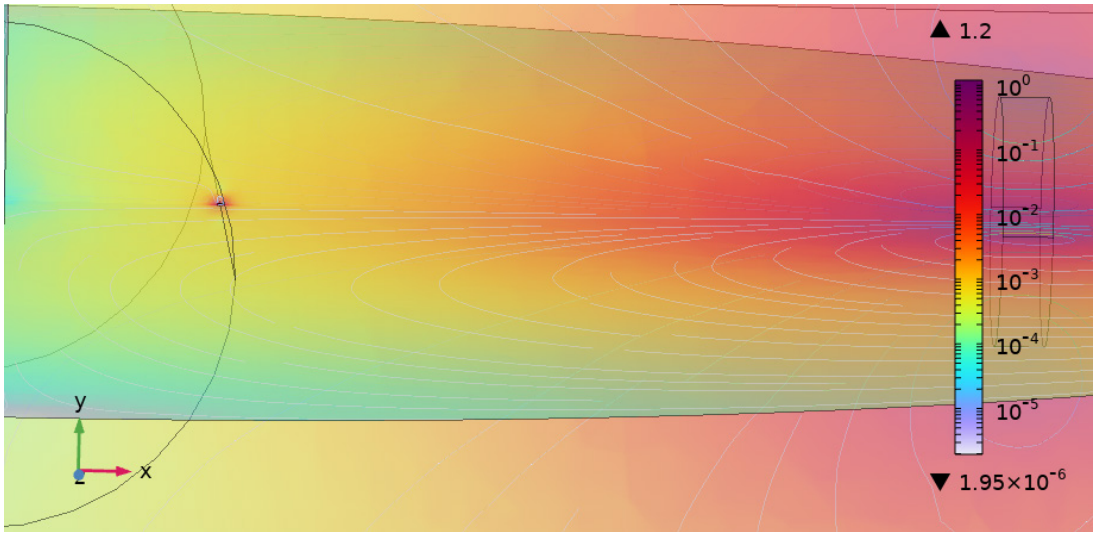

Figure 9 – When large permanent magnets move away, small permanent magnets remain at the boundary.

7. ANALYSIS OF SIMULATION EXPERIMENT RESULTS

Through simulation experiments, we can clearly see the magnetic field strength distribution of the magnetic stereotaxic system in three-dimensional space, and when the large permanent magnet on one side is moved, the external magnetic field changes significantly, thus providing a theoretical basis for the magnetic stereotaxic system. And it is found that when the large permanent magnet gradually approaches the center of three-dimensional space, the magnetic field around the implant (small permanent magnet) changes, causing the small permanent magnet to move towards the boundary position, which provides a theoretical basis for subsequent experiments.

Arduino controlled slide rail system

In the computer simulation experiment, we can clearly see that when the large permanent magnet on one side moves, the external magnetic field of the magnetic stereotaxic system changes significantly, so in the simulation experiment, we need to form a platform that can carry the large permanent magnet to move, and realize the precise control of the platform movement through the controller.

We chose a ball screw slide[15] with a stepper motor with a running distance of 300mm, a screw

accuracy of 0.05mm, and a 57x56 stepper motor[16] for the slide rail. Stepper motors[17] have four wires, they need to be connected to the stepper motor controller, the red wire is connected to A+, the green wire is connected to A-, the yellow wire is connected to B+, and the blue wire is connected to B-. The V+ of the external power supply is connected to the V+ of the stepper motor controller, and the V- of the external power supply is connected to the GND of the stepper motor controller. After that, the stepper motor controller is connected to the Arduino microcontroller[18-20] by prototype connection (i.e., PUL+ DIR+ENA+ in series, then connected to the 5V power pin of the Arduino, PUl-DIR - connected to the control pin of the Arduino board, respectively, and ENA - connected to the GND pin of the Arduion.), and then connect the Arduino controller to the computer through the data cable. At this point, a slide rail system controlled by the Arduino controller is completed.

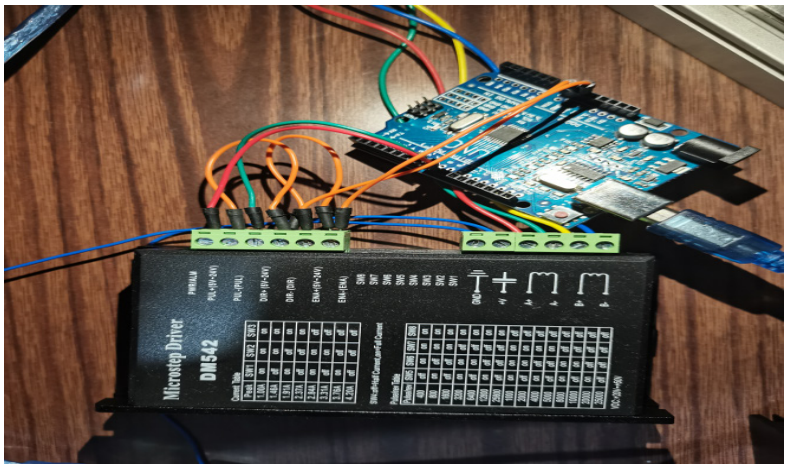

Figure 10 – Stepper motor controller with Arduino microcontroller

Since the external magnetic field of the magnetic stereotaxic system consists of four large permanent magnets, and in order to facilitate the operation of the slide rail system, we have built four slide system (i.e., the four large permanent magnets are equipped with four slide rails, each controlled by four Arduino controllers).

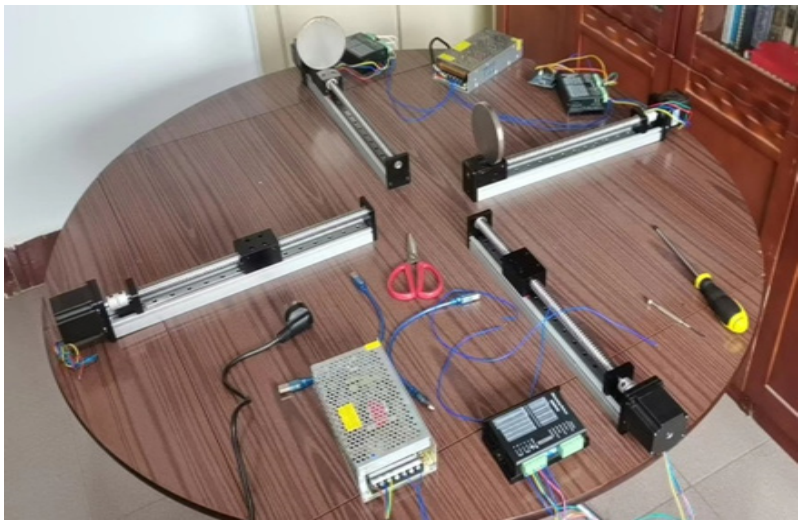

Figure 11 – External magnetic field control system for magnetic stereotaxic system.

We use 5% gelatin solution to simulate the working environment of the implant, pour the gelatin powder into a container, add a large amount of cold water to soak for 2 hours, then brew with hot water at 60-80 degrees Celsius, stirring until the gelatin is completely dissolved. Pour the dissolved gelatin solution into a transparent container with a diameter of 20 [cm], let it stand for a period of time, wait for the gelatin solution to become jelly-like, connect the small permanent magnet with a catheter, and put it in the center of the container. After that, the power is turned on and the slide rail system starts running.

After pre-setting the program on the computer, after the power is turned on, the slide rail system with a large permanent magnet on one side begins to move. At intervals, start the slide rail system on the adjacent side and repeat until all slide systems are fully operational. At this point, four large permanent magnets begin to

approach the container containing the gelatin solution sequentially. The first large permanent magnet gradually approaches the outer wall of the container, and the small permanent magnet is affected by its magnetic field, moves towards the first large permanent magnet, and stays on the inner wall of the container after being blocked by the container.

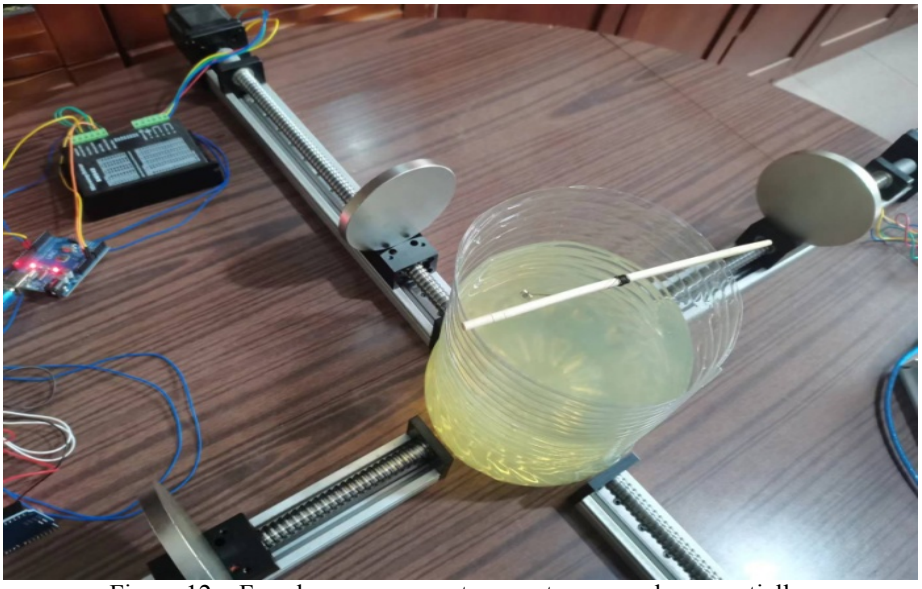

Figure 12 – Four large permanent magnets approach sequentially.

After the first large permanent magnet reaches the outer wall of the container, it begins to move in the opposite direction, and the small permanent magnet stays on the inner wall of the container. At this time, the second large permanent magnet gradually approached the outer wall of the container, and the small permanent magnet was affected by its magnetic field, began to move towards the second large permanent magnet, and after being blocked by the container again, stayed on the inner wall of the container close to the position of the second large permanent magnet.

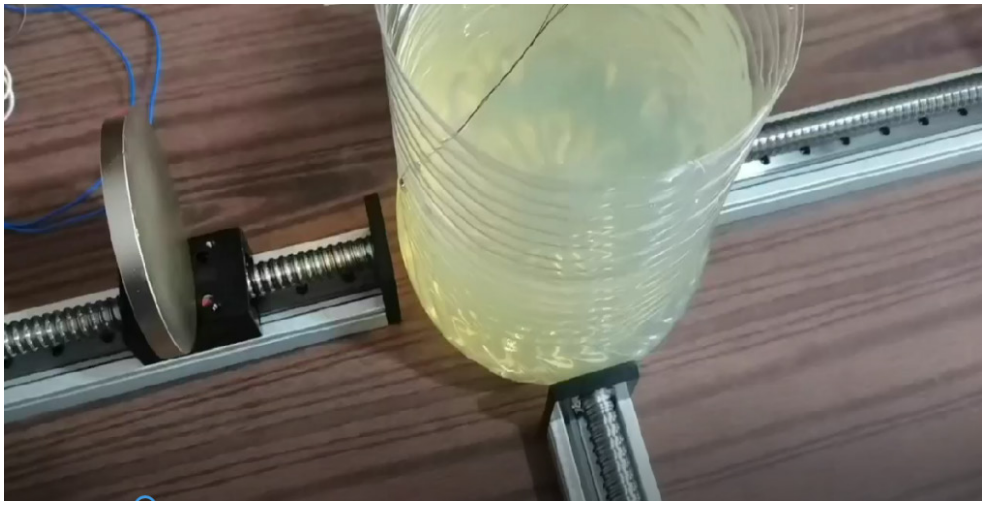

Figure 13 – When large permanent magnets move away, small permanent magnets stay at the boundary position.

When the second large permanent magnet begins to move in the opposite direction, the small permanent magnet remains on the inner wall of the container close to the second large permanent magnet. The third large permanent magnet begins to gradually approach, and the small permanent magnet, affected by its magnetic field, begins to move towards the third large permanent magnet until it is blocked by the container. The third large permanent magnet begins to move in the opposite direction, and the small permanent magnet remains on the inner wall of the container near the location of the third large permanent magnet. At this time, the fourth large permanent magnet begins to gradually approach, and the small permanent magnet, affected by its magnetic field,

moves towards the fourth large permanent magnet until it is blocked by the container and stays on the inner wall of the container. The fourth large permanent magnet began to move in the opposite direction, and the small permanent magnet remained on the inner wall of the container near the location of the fourth large permanent magnet.

8. EXPERIMENTAL CONCLUSIONS

Through simulation experiments, we find that in the magnetic stereotaxic system, changing the position of the large permanent magnet can change the external magnetic field, and the small permanent magnet can be displaced by the change of the external magnetic field. With the "Force Calculation" module in the COMSOL software, the attraction of large permanent magnets in different positions to small permanent magnets located in the center is obtained. At the same time, through the analysis of the magnetic field strength change of large permanent magnets, we find that when large permanent magnets are close to the center of three-dimensional space, the small permanent magnets will leave from the center position and move towards the approaching large permanent magnets until they are blocked by the boundary and stay on the inner wall of the boundary. When the large permanent magnet begins to leave, the small permanent magnet remains on the inner wall of the boundary. This provides a theoretical basis for the non-contact control of implants by the magnetic stereotaxic system, and also provides theoretical support for subsequent practical experiments.

In practical experiments, we built four slide rail systems to carry four large permanent magnets, and the four slide rail systems were controlled individually by four Arduino microcontrollers, allowing them to operate independently. After that, we simulated it according to the simulation experiment results and extended it on the basis of it. In the simulation experiment, only one large permanent magnet was moved, but in the actual experiment, after the first large permanent magnet began to move towards the container containing the gelatin solution, every certain interval, the adjacent slide rail system on one side was activated, and the large permanent magnet on this side began to move towards the container until all the large permanent magnets moved towards the container at certain intervals. The small permanent magnet, after being affected by the magnetic field of the first large permanent magnet, begins to move to the first large permanent magnet, and stays on the inner wall of the container after being blocked by the container, and the first large permanent magnet begins to move in the opposite direction after reaching the outer wall of the container, and the small permanent magnet still stays on the inner wall of the container. At this time, the large permanent magnet on the adjacent side gradually approaches the outer wall of the container, and its magnetic field touches the small permanent magnet, and the small permanent magnet begins to move towards the large permanent magnet on this side until it is blocked by the container and stays on the inner wall of the container. After that, the third and fourth large permanent magnets move in the opposite direction after approaching, and the small permanent magnets will move towards them first until they are blocked by the container and stay on the inner wall of the container.

This not only proves the correctness of computer simulation experiments, but also proves that non-contact control of implants is feasible in magnetic stereotaxic systems. It provides a theoretical basis and an important experimental basis for the magnetic stereotaxic system. It represents the transformation of magnetic stereotaxic system from theoretical research to experimental research and development.

REFERENCES

1. M A. Howard, M, Mayberg, M S. Grady, et al. Magnetic stereotactic system for treatment delivery: U.S. Patent 5,125,888[P]. 1992-6-30.
2. M A. Howard, M, Mayberg, M S. Grady et al. Magnetic stereotactic system for treatment delivery: U.S. Patent 5,779,694[P]. 1998-7-14.
3. M A. Howard, M, Mayburg, M S. Grady et al. Magnetic stereotactic system for treatment delivery: U.S. Patent 6,216,030[P]. 2001-4-10.
4. O. Avrunin, M. Tymkovych, V. Semenets, & V. Piatykop. (2019). Computed tomography dataset analysis for stereotaxic neurosurgery navigation. Paper presented at the Proceedings of the International Conference on Advanced Optoelectronics and Lasers, CAOL, , 2019-September 606-609. doi:10.1109/CAOL46282.2019.9019459
5. O. G. Avrunin, M. Alkhorayef, H. F. I Saied, & M. Y. Tymkovych, (2015). The surgical navigation system with optical position determination technology and sources of errors. Journal of Medical Imaging and Health Informatics, 5(4), 689-696. doi:10.1166/jmihi.2015.1444
6. Experimental study of the magnetic stereotaxis system for catheter manipulation within the brain / Grady M.S., Howard M.A., Dacey R.G. , Blume W., Lawson M., Werp P., Ritter R.C. // J. Neurosurg.– 2000.– Vol. 93, № 2.– P. 282–288.

7. O. G. Avrunin, M.Y. Tymkovych, S.P. Moskovko, etc.. (2017). Using a priori data for segmentation anatomical structures of the brain. PrzegladElektrotechniczny, 93(5), 102-105. doi:10.15199/48.2017.05.20
8. R. G. McNeil, R. C. Ritter, B. Wang, M. A. Lawson, G. T. Gillies, K. G. Wika, et al., "Functional design features and initial performance characteristics of a magnetic-implant guidance system for stereotactic neurosurgery", IEEE Trans. Biomed. Eng., vol. 42, pp. 793-801, Aug. 1995.
9. R W. Pryor. Multiphysics modeling using COMSOL®: a first principles approach[M]. Jones & Bartlett Publishers, 2009.
10. C. Multiphysics Introduction to COMSOL multiphysics®[J]. COMSOL Multiphysics, Burlington, MA, accessed Feb, 1998, 9: 2018.
11. Samoh A, Niamjan N, Yaiprasert C, et al. Comsol simulations of magnetic flux generated by permanent magnets with ring geometries[J]. Journal of Science and Arts, 2019, 19(3): 775-782.
12. O. G. Avrunin, Y. V Nosova,.etc. (2021). Possibilities of automated diagnostics of odontogenic sinusitis according to the computer tomography data. Sensors (Switzerland), 21(4), 1-22. doi:10.3390/s21041198
13. J. Hunkun and O. Avrunin, "Possibilities of Field Formation by Permanent Magnets in Magnetic Stereotactic Systems," 2022 IEEE 3rd KhPI Week on Advanced Technology (KhPIWeek), Kharkiv, Ukraine, 2022, pp. 1-4, doi: 10.1109/KhPIWeek57572.2022.9916450.
14. J. C. Maxwell. VIII. A dynamical theory of the electromagnetic field[J]. Philosophical transactions of the Royal Society of London, 1865 (155): 459-512.
15. M.F, Zaeh T. Oertli, J. Milberg. Finite element modelling of ball screw feed drive systems[J]. CIRP Annals, 2004, 53(1): 289-292.
16. Jr. R. Pulford Linear stepper motor: U.S. Patent 6,756,705[P]. 2004-6-29.
17. Defoort M, Nollet F, Floquet T, et al. A third-order sliding-mode controller for a stepper motor[J]. IEEE Transactions on Industrial Electronics, 2009, 56(9): 3337-3346.
18. L. Louis. working principle of Arduino and using it[J]. International Journal of Control, Automation, Communication and Systems (IJCACS), 2016, 1(2): 21-29.
19. Y. A. Badamasi The working principle of an Arduino[C]//2014 11th International Conference on Electronics, Computer and Computation (ICECCO). IEEE, 2014: 1-4.
20. A. A. Galadima Arduino as a learning tool[C]//2014 11th International Conference on Electronics, Computer and Computation (ICECCO). IEEE, 2014: 1-4.
21. Valentina Vassilenko, Anna Poplavska, Sergiy Pavlov, and etc. "Automated features analysis of patients with spinal diseases using medical thermal images", Proc. SPIE 11456, Optical Fibers and Their Applications 2020, 114560L (12 June 2020); https://doi.org/10.1117/12.2569780/

Надійшла до редакції 25.03.2023р.

HUNKUN JIAO - M.Sc., Kharkiv National University of Radio Electronics, Kharkiv, 61166, Ukraine, ***e-mail: 1350829683@qq.com,***

AVRUNIN OLEH - D. Techn. Sc., Kharkiv National University of Radio Electronics, Kharkiv, 61166, Ukraine, ***e-mail:oleh.avrunin@nure.ua***

Цзяо ХАНКУНЬ, Олег АВРУНІН

ДОСЛІДЖЕННЯ ТА ТЕХНІКО-ЕКОНОМІЧНЕ ОБҐРУНТУВАННЯ ВИКОРИСТАННЯ МАГНІТНОЇ СТЕРЕОТАКСИЧНОЇ СИСТЕМИ

Харківський національний університет радіоелектроніки